Conformation of Sulfoquinovosyldiacylglycerol Bound to a Magnetically Oriented Membrane System

Kathleen P. Howard and James H. Prestegard
Department of Chemistry, Yale University, New Haven, Connecticut 06511 USA

ABSTRACT The conformation of uniformly ^{13}C-labeled sulfoquinovosyldiacylglycerol (SQDG) is studied in both membrane and solution environments using NMR spectroscopy. Analysis in a membrane-like environment is based on the measurement of dipolar interactions between ^{13}C-^{13}C and ^{1}H-^{13}C spin pairs and on the measurement of ^{13}C chemical shift anisotropy offsets, which appear in magnetically oriented phospholipid-based membrane fragments. Potential energy maps for glycosidic torsions, ϕ, ψ, and $\theta 1$, are calculated with a membrane interaction energy and are used in the interpretation of experimental data. The membrane-bound description for SQDG is most consistent with a set of low-energy conformations that extends the headgroup of SQDG away from the membrane surface. Analysis of the conformation of SQDG in CD_3OD solution is based on measured $^3J_{CH}$ scalar couplings. The description of the solution conformation is modeled as a mixture of low-energy conformers predicted in the absence of a membrane interaction term and involves more extensive motional averaging than the model for SQDG embedded in the lipid matrix.

INTRODUCTION

Sulfoquinovosyldiacylglycerol (SQDG), commonly referred to as the "plant sulfolipid," was first discovered by Benson and co-workers in 1959 and has since been found to exist in all photosynthetic organisms (Benson et al., 1959). The chemical structure of the lipid in shown in Fig. 1. In contrast to most naturally occurring organosulfur compounds (including sulfur containing lipids), where sulfur occurs in a sulfate ester (C-O-SO_3^-), SQDG contains a sulfonic acid group in which the carbon at the six position of glucose is directly bonded to sulfur. Sulfonic acids of this type are chemically very stable and strongly acidic (Barber and Gounaris, 1986; Harwood, 1980).

SQDG is an intriguing lipid, not only because of its unusual chemical structure, but also because of its role is still poorly understood. Various functions have been postulated for SQDG, but in most cases the data are sparse and are not definitive. It has been proposed that SQDG is closely associated with protein complexes (Gounaris and Barber, 1985; Pick et al., 1985), where it is tightly bound and participates in either catalytic activities or in maintaining the complexes in a functional conformation. The association is probably partly stabilized by electrostatic interactions between its negatively charged sulfonate group and positive charges within the proteins. In some cases the interactions may be very strong, as suggested by the resistance of some SQDG molecules bound to chloroplast ATP synthase (CF_0-CF_1) to exchanging with other lipids (Pick et al., 1985).

SQDG has also attracted interest because of its potential inhibition of the AIDS virus. Taking advantage of a newly developed soluble formazan assay to screen for the cytopathic effects of HIV-1 (Weislow et al., 1989), scientists at the National Cancer Institute identified SQDG as a potential inhibitor of HIV-1 while screening a series of isolates from cyanobacterial media. In light of its activity and undetermined mechanism of action, SQDG was selected as a high priority for further investigation and evaluation for possible clinical usefulness against AIDS (Gustafson et al., 1989). Recently a synthetic route to the cyanobacterial sulfolipid was developed in response to its potential clinical value (Gordon and Danishefsky, 1991). Several retroviruses, including HIV-1, have been reported to bind sulfated polysaccharides (McAlarney et al., 1994; McClure et al., 1992; Van den Berg et al., 1992), and it is possible that SQDG interferes with viral recognition of cell-surface receptors. Although there have been several reports on the physical properties of SQDG (Johns et al., 1978), the molecular details of the conformation of SQDG bound at a membrane surface have not been described.

Studying glycolipids within a lipid lattice presents serious obstacles for the application of the most widely used methods of structural biology. Membrane systems have proved difficult to crystallize for use in x-ray diffraction studies. The few x-ray crystal structures of isolated glycolipids that do exist are useful in showing possible minimum energy structures for these molecules. However, packing constraints on headgroups may induce changes in the backbone and acyl chain conformations that are not present in the physiologically relevant liquid crystalline phase (Pascher et al., 1992). Solution-state nuclear magnetic resonance (NMR) has been used to study membrane-bound glycolipids incorporated into small micelles or unilamellar vesicles, but the broad linewidths and efficient spin diffusion that accompany the relatively slow reorientation of micelle complexes complicate structural analysis (Siebert et al., 1992).

Received for publication 1 September 1995 and in final form 1 August 1996.

Address reprint requests to Dr. James H. Prestegard, Department of Chemistry, Yale University, P.O. Box 6666, New Haven, CT 06511-8118. Tel.: 203-432-5162; Fax: 203-432-8918; E-mail: jhp@psun.chem.yale.edu.

Dr. Howard's present address is Department of Chemistry, University of Pennsylvania, Philadelphia, PA 19104.

0006-3495/96/11/2573/10 $2.00

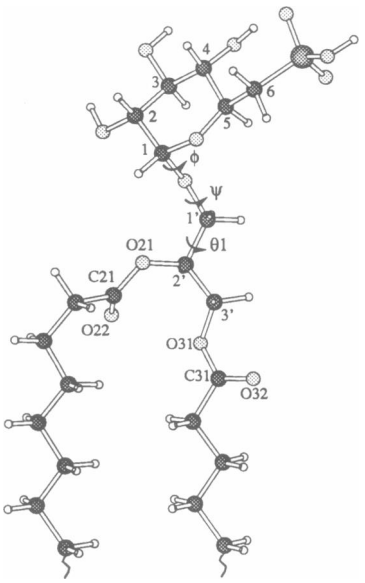

FIGURE 1 Atom numbering and torsion labeling for SQDG. θ = O5-C1-O1-C1′; ψ = C1-O1-C1′-C2′; $\theta 1$ = O1-C1′-C2′-C3′.

The most relevant structural and dynamic data on glycerolipids is derived from studies in liquid crystalline bilayers. Solid-state NMR techniques have proved to be particularly useful in the study of phospholipids (Braach-Maksvytis and Cornell, 1988; Smith et al., 1992; Strenk et al., 1985) and glycolipids (Auger et al., 1990; Jarrell et al., 1987; Skarjune and Oldfield, 1982). More recently, we have developed methodology utilizing magnetically oriented phospholipid bilayers to study the conformation of membrane-bound molecules using orientational constraints derived from dipolar and quadrupolar couplings and chemical shift anisotropy data (Sanders et al., 1994). This methodology has been used to study the membrane-bound orientations of glycolipids prepared by synthetic methods with isotopic labels (^{13}C, ^{2}H) at specific sites (Aubin et al., 1993; Hare et al., 1994; Sanders and Prestegard, 1991, 1992). In addition, we have successfully applied this methodology to uniformly ^{13}C-labeled diacylglycerol glycolipids isolated from algal extracts. We have reported detailed NMR studies of two abundant glycolipids found in photosynthetic membranes, monogalactosyldiacylglycerol (MGDG) (Howard and Prestegard, 1995) and digalactosyldiacylglycerol (DGDG) (Howard and Prestegard, 1996). Here we apply the methodology to study another member of the diacylglycerol glycolipid class.

The orientation of the saccharide headgroup of SQDG is primarily determined by the conformation of the linkage between the headgroup and the glycerol moiety (torsion angles ϕ, ψ, $\theta 1$ in Fig. 1). In this study, models defined by average torsions about ϕ, ψ, and $\theta 1$, and motion about these averages, are derived from the NMR data and compared with results from molecular modeling. The modeling protocol used here for comparison to models from experimental membrane data includes a membrane interaction energy. Several studies have suggested that the membrane surface considerably reduces the range of possible conformations for the saccharide-lipid linkage (Howard and Prestegard, 1995; Nyholm and Pascher, 1993; Ram et al., 1992; Winsborrow et al., 1992). In modeling membrane effects we have adopted a rather simple procedure that represents the membrane as a smooth transition from a low-dielectric, low-surface, free energy medium (ϵ = 4) to a high-dielectric, high-surface, free energy medium (ϵ = 80). Interaction energy contributions for membrane-anchored molecules are calculated as the sum of interfacial and reaction field terms. These energy contributions are easily incorporated into standard molecular mechanics programs (Ram et al., 1992). For comparison of membrane conformational properties to those found in solution, the conformation of SQDG in solution is derived from the measurement of three-bond heteronuclear scalar couplings ($^{3}J_{CH}$) and analyzed without the use of a membrane interaction term.

MATERIALS AND METHODS

Materials

3-[(Cholamidopropyl)dimethylammonia]-2-hydroxyl-1-propanesulfonate (CHAPSO) and L-α-dimyristoylphosphatidylcholine (DMPC) were purchased from Sigma Chemical Company (St. Louis, MO). Uniformly ^{13}C-labeled (~26%) algal extracts were obtained from Cambridge Isotopes (Andover, MA), and ^{13}C-labeled SQDG, also known as [1,2-di-acyl-3-(6-sulfo-α-D-quinovopyranosyl)-*sn*-glycerol], was isolated from these algal extracts using flash chromatography on a series of silica gel columns. Elution was with 13:7:1 (chloroform/methanol/ammonium hydroxide) and 91:30:6:2 (acetone/toluene/water/acetic acid) (Sato and Murata, 1988). All reagents used in the purification of SQDG or the preparation of NMR samples were purchased from either Sigma Chemical Company (St. Louis, MO) or Aldrich Chemical Company (Milwaukee, WI).

Preparation of NMR samples

Liquid crystalline NMR samples composed of arrays of bilayer disks were prepared directly in 5 mm NMR tubes. A complete description of the oriented DMPC/CHAPSO system has been published elsewhere (Sanders et al., 1994; Sanders and Prestegard, 1990). Briefly, ~10 mg of 26% uniformly ^{13}C-labeled SQDG, 107 mg DMPC, and 33 mg of CHAPSO were mixed in 350 μl of buffer (0.1 M NaCl, 1 mM dithiothreitol, 50% D_2O, 50% H_2O) by a combination of centrifugation, heating, cooling, and sonication until a homogeneous sample was obtained. This mixture represents a mole fraction composition of 1/0.33/0.06 for DMPC/CHAPSO/SQDG. At 30% w/v lipid content, the samples spontaneously form an oriented liquid crystalline phase when placed in a magnetic field. Samples were diluted to a lipid content of 20% to induce isotropic tumbling for the determination of the signs of dipolar couplings and isotropic chemical shifts.

NMR spectroscopy

Solution spectra were collected on either a Bruker AM-500 spectrometer or a GE Omega 500 spectrometer (125.76 MHz for ^{13}C, 500 MHz ^{1}H). A ^{1}H double-quantum filtered correlation experiment (DQFCOSY) (Rance et al., 1983) was used to assign proton resonances of SQDG. Heteronuclear multiple quantum coherence (HMQC) (Bax et al., 1983) and heteronuclear multiple bond correlation (HMBC) (Bax and Summers, 1986) spectra correlated ^{1}H and ^{13}C resonances and provided assignments of ^{13}C reso-

nances. Taking advantage of the ^{13}C enrichment, assignments were verified using a three-dimensional ^{1}H-detected ^{13}C-^{13}C COSY (Gosser et al., 1993). These were in close agreement with those previously reported in the literature (Johns et al., 1978). Assignments of carbon resonances of SQDG in the oriented membrane samples were based on analogy to solution data and reinforced by connectivities observed in the ^{13}C-^{13}C correlation experiments under oriented conditions.

All oriented spectra were collected unlocked and without sample spinning. ^{31}P-^{1}H decoupled spectra for the estimation of $S_{bilayer}$ were collected on a GE Omega 300 spectrometer (121 MHz for ^{31}P). ^{13}C oriented spectra were collected on a Bruker AM 500 using a standard 5-mm ^{13}C-^{1}H dual probe (^{13}C 90 pw $\approx$ 6.2 us; ^{1}H 90 pw $\approx$ 26 us). ^{1}H decoupling was effected using WALTZ (Shaka et al., 1983) with maximum available (40 W) decoupling power only during acquisition. To avoid sample heating due to high decoupling levels, acquisition times were limited to about 40 ms with delays of approximately 1.5 s between acquisitions. For sensitivity enhancement through the nuclear Overhauser effect, ^{13}C spectra were collected with low-power (0.3 W) decoupling during the predelay. Spectral widths for ^{13}C spectra were commonly 25,000 Hz. ^{13}C free induction decays were generally collected with 1K points, zero filled to 2K points, and then exponentially multiplied with 10-Hz line broadening (20-Hz line broadening for ^{13}C-^{1}H coupled spectra).

^{13}C-^{13}C dipolar couplings for SQDG were measured using ^{1}H-decoupled ^{13}C-^{13}C DQFCOSY (Rance et al., 1983) and 2D INADEQUATE (incredible natural abundance double-quantum transfer experiment) (Mareci and Freeman, 1982). For both DQFCOSY and 2D INADEQUATE experiments, 128 t1 points were collected with approximately 1024 scans per experiment (at least 48 h total acquisition). The sweep widths were generally 26,000 Hz in t2 and 8500 Hz in the t1 dimension.

$^{3}J_{CH}$ were measured using a 2D heteronuclear single-quantum coherence experiment (HSQC) optimized to detect long-range heteronuclear couplings (Bodenhausen and Ruben, 1980), following the same procedure as previously reported (Howard and Prestegard, 1995).

Analysis of anisotropic spectral parameters

Both dipolar couplings and chemical shift anisotropies are a source of structural and dynamic information in anisotropic media. Dipolar couplings, $D_{i,j}$ (Hz), may be written as follows:

$$D_{ij} = \left(\frac{\mu_0}{4\pi}\right)\frac{-\gamma_i\gamma_j h}{2\pi^2 r^3} S_{system} S_{mol}\left(\overline{\frac{3\cos^2\theta - 1}{2}}\right), \qquad (1)$$

where γ_i and γ_j are the gyromagnetic ratios of the two interacting nuclei, h is Planck's constant, r is the distance between coupled nuclei, and θ is the angle between the internuclear vector i-j and the bilayer normal (Harris, 1983). Net orientation and motion of the bilayer discs that comprise the liquid crystalline assemblies are included in a single-order parameter, S_{system}, that scales all spectral parameters. S_{system} is defined as

$$S_{system} = -\frac{1}{2} S_{bilayer}, \qquad (2)$$

where the factor of $-1/2$ arises from the fact that DMPC bilayer discs orient with their normals at 90° relative to the field and rotate rapidly about this axis. The bilayer disks also wobble about the average orthogonal direction in an axially symmetrical fashion. $S_{bilayer}$ describes the residual order of the bilayer normal axes in comparison to a fully extended bilayer membrane ($S_{bilayer} = 0.65$). $S_{bilayer}$ is based on the anisotropic ^{31}P shift of DMPC comprising the bulk of our lipid matrix relative to the ^{31}P shift seen in multilayer dispersions. Over and above S_{system}, experimental splittings are reduced by local molecular motions relative to the bilayer normal. S_{mol} is an order parameter assigned to account for reduction of couplings due to axially symmetrical motion of the membrane anchor of SQDG. (Although the assumption of axially symmetrical averaging is an oversimplification, the approximate cylindrical shape of SQDG suggests relatively unhindered rotation and oscillation about the most ordered director axis.) Further motion about glycosidic torsion angles that can scale down dipolar couplings measured for the headgroup are included in the average implied by the bar over the angular term in Eq. 1. Torsion angle analysis (Hare et al., 1993) is used to find a description for the conformation and dynamics of the headgroup of SQDG in terms of average glycosidic torsions and motion about these torsions. A full description of the analysis is provided in the Results.

Carbonyls at the ester linkages of SQDG have measurable chemical shift anisotropy offsets that can also provide useful conformational and dynamic information. The observed chemical shift in an anisotropic system shows a dependence on order and molecular orientation which is very similar to that for dipolar coupling described above (Howard and Prestegard, 1995; Sanders et al., 1994).

Molecular modeling

Conformational energy maps as a function of the torsion angles of the saccharide-glycerol linkage (ϕ, ψ, and $\theta 1$) were calculated with AMBER 4.0 modified to include a membrane interaction energy (Ram et al., 1992). A starting conformation for SQDG was modeled by linking the crystal structure of the anhydrous rubidium salt of deacylated SQDG (Okaya, 1964) to the diacylglycerol moiety of a low-energy structure for DMPC. The DMPC structure was calculated (molecule 2, DMPC2 for Vanderkooi, 1991) using energy minimization of the DMPC-$2H_2O$ crystal (Pearson and Pascher, 1979). In the crystal structure for the headgroup of SQDG, the sulfonic acid group is bent back toward the sugar (H5-C5-C6-S = −63.5°). However, vicinal coupling constants measured for SQDG in CD_3OD solution ($^{3}J_{HH}$ H5-H6′ = 6.3; $^{3}J_{HH}$ H5-H6 = 5.1) are more consistent with a equilibrium between nearly equal populations of two *gauche* conformers about H5-C5-C6-S. For membrane conformation analysis therefore, the H5-C5-C6-S torsion was rotated to 60°, which led to less steric hindrance between the headgroup and the backbone/surface of the membrane for most ϕ, ψ, and $\theta 1$ combinations. Three families of structures (one for each of the staggered conformations of $\theta 1$) were generated by rotation of the ϕ and ψ torsion angles at 20° intervals using the MULTIC option of MacroModel V3.1 (Still, 1990). Energy minimization was performed at each grid point to generate relaxed energy maps. Minimization included all degrees of freedom, except for the torsion angles defining the respective grid point. After 5000 cycles of steepest descent, conjugate gradient minimization was used to achieve the convergence criterion of 0.05 kcal/mol. A force field with improved parameterization for oligosaccharides was utilized (Scarsdale et al., 1988). Molecular modeling of SQDG required parameterization of the sulfonic acid moiety. Changes made to the all-atom force field of AMBER are noted in Table 1. A new atom type was introduced for the sulfonic acid sulfur (SA). All other atom types that appear in the new bond length, bond angle, and torsional parameters were taken from existing atom types in the force field (Weiner et al., 1984, 1986). The equilibrium bond lengths and bond angles for the sulfonic acid group were taken from x-ray data (Lamba et al., 1994; Okaya, 1964). Force constants were based on parameterization of sulfated monosaccharides (Kogelberg and Ruitherford, 1994) and are similar to related parameters for the phosphate group in the AMBER force field (Weiner, 1984). The van der Waals parameters for SA were taken to be the same as for S in the all-atom force field (Weiner et al., 1984, 1986). Partial charges were assigned based on an AMPAC calculation of a sulfated monosaccharide (Kogelberg and Ruitherford, 1994) and are consistent with bond moments for C-S and S=O from related compounds (Allinger and Kao, 1976). Because of our primary interest in conformation about the glycosidic link, and a lack of experimental NMR data on the conformation of the sulfonic acid moiety, a more rigorous parameterization was not deemed necessary.

RESULTS

Fig. 2 is the ^{1}H-decoupled ^{13}C spectrum of 26% uniformly ^{13}C-labeled SQDG in DMPC/CHAPSO under conditions where orientation is achieved. The sugar and glycerol res-

TABLE 1 Parameterization of sulfonic acid moiety of SQDG

New atom type	Mass		
SA	32.060		
Bond type	K_r(kcal mol^{-1} Å^{-2})	r_{eq} (Å)	
CT-SA	222	1.77	
SA-O2	525	1.44	
SA-OH	260	1.58	
Angle type	K_θ (kcal mol^{-1} rad^{-2})	θ_{eq} (°)	
CT-SA-O2	55	106.0	
O2-SA-OH	75	113.5	
CT-SA-OH	55	105.0	
O2-SA-O2	118	110.0	
SA-OH-HO	55	108.0	
CT-CT-SA	80	117.0	
HC-CT-SA	35	109.5	
Torsion type	Vn/2 (kcal mol^{-1})	γ(°)	n
X-CT-SA-X	0.750	0.0	3.0
X-SA-OH-X	0.750	0.0	3.0
van der Waals terms			
Atom type	R^*(Å)	ε (kcal/mol)	
SA	2.00	0.20	

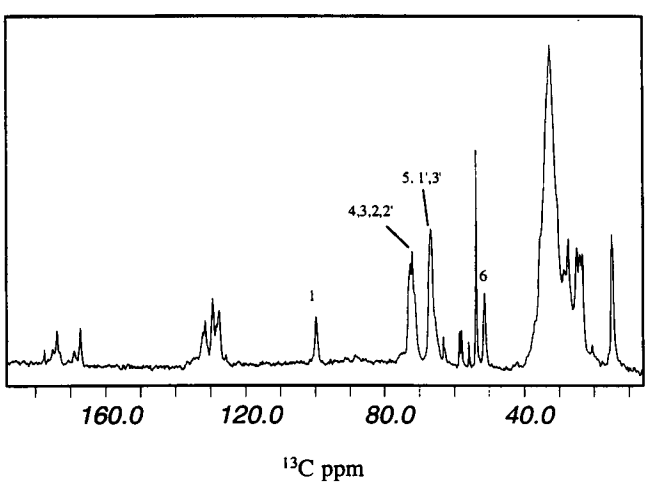

FIGURE 2 ^{13}C-^{1}H decoupled spectrum of 10 mg 26% ^{13}C SQDG in 30% w/v DMPC/CHAPSO 3:1 at 303°K. Sugar and glycerol resonances are labeled.

onances are labeled. With the exception of the well-resolved C1 and C6 sugar resonances, the five other sugar resonances and three glycerol peaks are in the crowded region between 60 and 75 ppm. With the exception of some unsaturated sites near 130 ppm, most acyl chain resonances are far upfield (<40 ppm). The carbonyl region has five peaks: one from CHAPSO (177.5 ppm), two relatively sharp peaks from the DMPC carbonyls (174.4 and 167.8 ppm), and two broad peaks from the SQDG carbonyls (175.7 and 170.2 ppm). Comparing Fig. 2 with the spectrum of the same sample under isotropic conditions permitted measurement of the chemical shift anisotropy (CSA) offsets. Under isotropic conditions both DMPC carbonyl peaks and both SQDG carbonyl peaks fall under a broad peak at 174.4 ppm. The CSA offsets for the SQDG carbonyls are thus +1.3 ± 1.0 and −4.2 ± 1.0 ppm. These values differ from those observed for the two diacylglycerol glycolipids previously studied (Howard and Prestegard, 1995, 1996) and will be discussed more fully below.

Interference from peaks from isolated ^{13}C sites from SQDG and from natural abundance sites in the supporting membrane matrix prevents measurement of dipolar ^{13}C-^{13}C couplings directly from the data in Fig. 2. ^{13}C-^{13}C dipolar couplings were therefore measured using two-dimensional double-quantum filtered spectroscopy (DQFCOSY and 2D INADEQUATE), which removes the signal from isolated ^{13}C nuclei. All couplings resolved involved one or the other of the well-resolved C1 or C6 resonances. Slices from a 2D INADEQUATE optimized for $(J + D)$ = 200 Hz are shown in Fig. 3. Couplings were measured as splittings of the antiphase pairs of resonances. In addition to the directly bonded C1-C2 coupling (|164| ± 40 Hz) and C5-C6 coupling (|102| ± 40 Hz), Fig. 3 shows a well-resolved long-range coupling between C4 and C6 (|100| ± 40 Hz). Not shown in Fig. 3, but resolved in both DQFCOSY and 2D INADEQUATE spectra, was another long-range coupling (|130| ± 40 Hz) between C1 and C1′, the first carbon of the glycerol backbone. The C1-H1 coupling (−1212 ± 150 Hz) was also measured from the ^{1}H-coupled version of Fig. 2. The sign of the C1-H1 coupling was determined based on the temperature dependence of the coupling in a series of ^{1}H-coupled ^{13}C spectra of 26% ^{13}C SQDG in 20% w/v DMPC/CHAPSO. As the temperature is decreased from 305°K to 292°K, the sample gradually looses its orientation and becomes isotropic. As this occurs, the C-H coupling

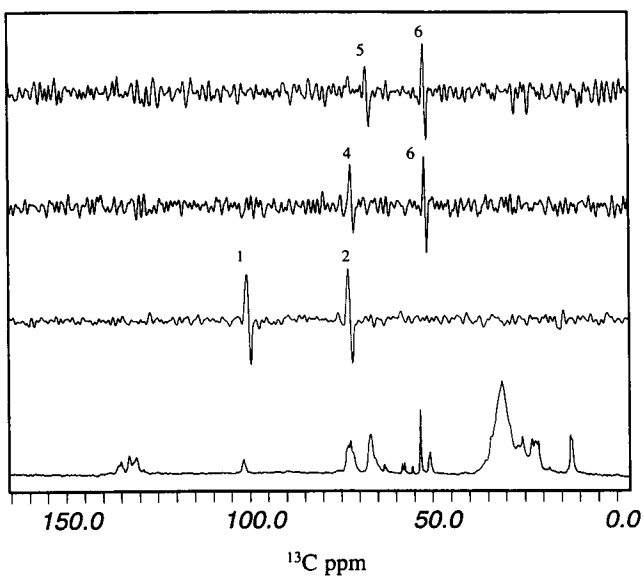

FIGURE 3 D2 slices from a 2D INADEQUATE (125.76 MHz) of the sample described in Fig. 2 optimized for $(J + D)$ = 200 Hz. The spectrum was processed using sinebell multiplication in both dimensions.

passes through a minimum and then splits to reach a 150-Hz purely scalar coupling at 292°K. This suggests that dipolar and scalar contributions to the splitting are of opposite sign, yielding a negative value for the C1-H1 dipolar coupling. Table 2 summarizes the dipolar couplings measured for membrane-bound SQDG.

Analysis of headgroup data

Prospects for analysis of the conformational and dynamic properties of the sugar ring of SQDG are most promising because several measurable dipolar couplings (C1-H1, C1-C2, C5-C6, and C4-C6) are concentrated in a central ring that can be well approximated as a single rigid structure. Bond angles, internuclear distances, and orientations of exocyclic groups such as the C6 hydroxymethyl can be taken from structures optimized as described in the modeling section. Within the bounds of this assumed ring structure, the observed reduced values of the dipolar couplings can be viewed as the result of averaging about the glycosidic torsions, θ, ψ, and $\theta 1$, as well as the scaling due to axially symmetrical motion of the glycerol backbone to which the headgroup is attached (S_{mol}). The use of the single parameter S_{mol} to model the motion of the headgroup attachment site does require the choice of a director orientation within the glycerol backbone and in particular with respect to the C1′-C2′ bond that defines the headgroup $\theta 1$ rotation axis. As will be discussed after this section, we do not have sufficient data on the glycerol moiety itself to independently determine the orientation of the axis. For now we will assume it to lie along the γ-chain of the diacylglycerol backbone as it exists in the energy-minimized DMPC crystal structure (Vanderkooi, 1991; molecule 2, DMPC2). This conformation places the C1′-C2′ bond at an angle of about 30° to the director. (This angle is also very similar in the other molecule found in the crystal structure of DMPC.)

TABLE 2 Dipolar couplings measured for 26% ^{13}C-labeled SQDG dissolved in 30% w/v DMPC/CHAPSO 3:1 at 303°K

Dipolar couplings	Measured (Hz)	Corrected (Hz)*	Predicted (Hz)#
Headgroup			
C1-C2	|164| ± 40	119 ± 40	110
C5-C6	|102| ± 40	−147 ± 40	−142
C4-C6	|100| ± 45	−100 ± 40	−95
C1-H1	−1212 ± 150	−1381 ± 150	−1485
Headgroup to backbone			
C1-C1′	|130| ± 40	130 ± 40	123

*Corrected values have been adjusted to eliminate the effects of scalar coupling ($^1J_{C\text{-}C}$ = 45 Hz and $^1J_{C\text{-}H}$ = 169 Hz). The signed set that gave the best fit solutions is listed.

#The predicted values are a representative set from the best-fit solution family using a square well model for motional averaging of ϕ and Ψ and variable populations for the three minima for $\theta 1$. (ϕ = 65; Ψ = 105 (±30); $\theta 1$: ap = 100%; S_{mol} = 0.65.) The rmsd for the fit of the headgroup data is 0.009.

Dipolar couplings measured for the headgroup can always be expressed as averages of second-order spherical harmonics written in the laboratory frame. Wigner rotation matrices can then be used to transform the spherical harmonics from the laboratory frame through a set of frames that allows independent and uncorrelated averaging about the discrete glycosidic torsions, ϕ, ψ, and $\theta 1$ (Hare et al., 1993). The motions about ϕ and ψ are believed to be localized within single broad minima. Thus, torsional motion around these angles was modeled by using a simple square well potential. All angles within the allowed well were assumed to occur with equal probability. $\theta 1$ is believed to sample one or more rotational states, separated by approximately 120°. We therefore allowed sampling of three discrete wells and treated motion about $\theta 1$ as a weighted average over three low-energy staggered conformations (ap, sc, and −sc) (ap, anti-periplanar, 180° ± 30; sc, syn-clinal, 60° ± 30; −sc, −syn-clinal, −60° ± 30). Solutions for headgroup orientation and motion are therefore expressed as centers and well widths for ϕ and ψ and populations of the staggered conformations of $\theta 1$.

Conformations of the headgroup of SQDG consistent with measured dipolar couplings were found using a program written in C++ (Hare et al., 1993). Taking into account all possible sign combinations of dipolar couplings, eight signed sets were searched, varying S_{mol} between 0.2 and 0.7, with a root mean square deviation (rmsd) cutoff of 0.015. (Data were scaled by the maximum expected splitting scaled by S_{system} for normalization before calculation of rmsds.) Only one signed set gave solutions (see Table 2). The solutions for this set fell into two families, one centered at $\phi = 65/\psi = 105$ and the other at $\phi = 160/\psi = 215$ (see Fig. 4). Both families had a 100% population of the ap conformer of $\theta 1$ and extended the headgroup into the solvent with no obvious steric contacts with the backbone or

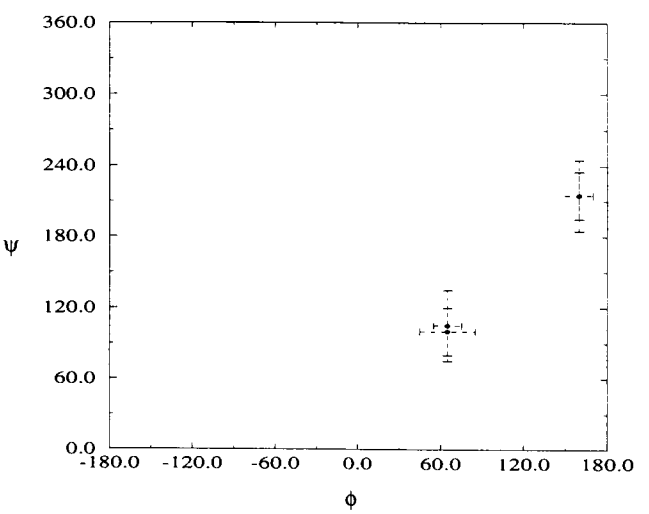

FIGURE 4 ϕ/ψ values for conformations of SQDG that fit the experimental data listed in Table 2 with rmsd less than 0.015. Dotted lines indicate the well widths over which ϕ and ψ are averaged.

membrane surface. Furthermore, both solution families had S_{mol} values in the range 0.6–0.71. The solution centered at $\phi = 65/\psi = 105$ does, however, extend further into the bulk solvent and falls into a lower energy region of a potential energy map calculated for SQDG as a function of ϕ and ψ (see Discussion). A stereo diagram of the best-fit solution from the $\phi = 65/\psi = 105$ family is shown in Fig. 5.

Analysis of diacylglycerol backbone data

As mentioned above, there are no adequate data to define a precise conformation of the glycerol backbone and headgroup attachment site (the C1′-C2′ vector). However, the S_{mol} value generated above is meant to account for motion of the backbone in the lipid matrix, and we can discuss the limited data we have in terms of consistency with this value. One of the pieces of data that reflects on backbone conformation is a measured C1-C1′ coupling between the backbone C1′ carbon and the headgroup C1 carbon. The average orientation and motional averaging of the vector connecting these carbons are affected by the ψ torsional averaging determined above, but also very directly by the motion of the C1′-C2′ vector of the glycerol backbone. Assuming no variations in the C1-O-C1′ bond angle, the distance between C1 and C1′ is fixed at 2.43 Å. The predicted dipolar coupling for C1-C1′ is 123 Hz for the $\phi = 65/\psi = 105 \pm 30$ solution and 93 Hz for the $\phi = 160/\psi = 215 \pm 30$ solution. Both fall marginally within experimental error (± 40 Hz, considered to be half a linewidth), but the solution centered at $\phi = 65/\psi = 105$ clearly agrees very well with the experimental value of 130 Hz. Hence there is some support for our initial choice of director as lying along the γ-chain of the diacylglycerol backbone.

CSA offsets measured for the carbonyl carbons of the attached acyl chains also provide some conformational information. However, the analysis is complicated by additional motional averaging about bonds attaching acyl chains to the glycerol backbone. In particular, motion about C2′-O21 and O21-C21 can contribute to averaging of the β-chain carbonyl CSA offset. Motion about C2′-C3′, C3′-O31, and O31-C31 can contribute to averaging of the γ-chain carbonyl offset. One simple approach would be to assume that motion about these bonds is of small amplitude and to anticipate that they may just provide a further scaling of predictions based on a rigid model for the backbone undergoing axially symmetrical averaging described by S_{mol}.

To quantitatively employ CSA data in structural studies, both the static tensor eigenvalues and the orientation of the eigenvectors within the molecular frame must be known. Although neither the magnitudes nor orientations for shift tensor principal values have been measured for SQDG, values derived from suitable model compounds can be used. The principal values of the ^{13}C carbonyl tensor were taken from the experimentally determined ^{13}C carbonyl chemical shift tensor for distearoyl phosphatidylcholine monohydrate (Cornell, 1980) and the principal axes from solid dimethy oxalate (Cornell, 1986). The orientation of the principal axes corresponding to σ_{22} and σ_{11} are in the plane containing C═O and C-O, with σ_{22} approximately along the C═O bond. The orientation of the principal axis corresponding to σ_{33} is nearly perpendicular to this plane.

Using the DMPC2 conformation from the energy-minimized DMPC crystal structure (Vanderkooi, 1991), and assuming the axis of motional averaging is along the long axis of the γ acyl chain, we searched for axially symmetrical order parameter values consistent with models for the headgroup conformation. The rigid model based on DMPC2 predicts signs for CSA offsets consistent with the observed offsets. However, even at the lower bound for headgroup S_{mol} values ($S_{mol} = 0.6$), the predicted CSA offsets for the backbone carbonyls are about 3.5 times larger (4.7 ppm, −14.6 ppm) than the experimental values (1.3 ± 1.0 ppm, −4.2 ± 1.0 ppm). A rigid model based on the other molecule found in the crystal structure of DMPC (DMPC1) also agrees qualitatively in terms of the relative sign and ampli-

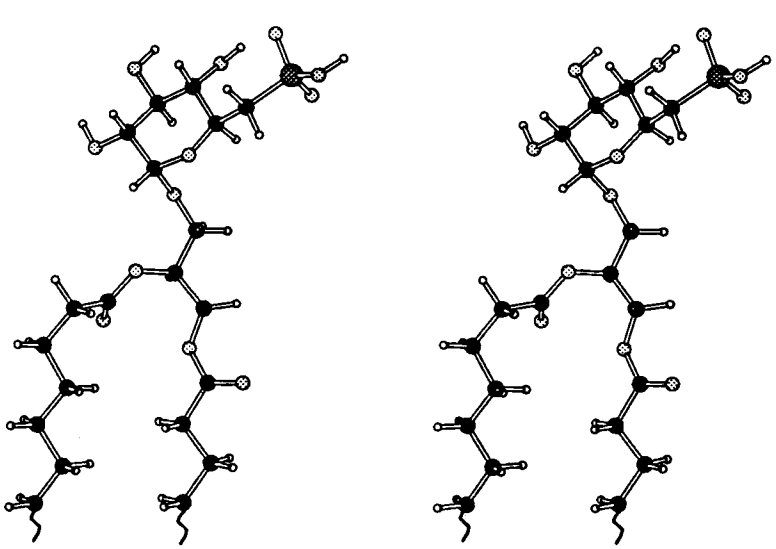

FIGURE 5 Stereo diagram of the best fit membrane-bound conformation for SQDG as described in footnote # of Table 2.

tude of the two predicted CSA offsets, but is even further off quantitatively. In our previously published NMR study of membrane-bound MGDG (Howard and Prestegard, 1995), we were able to use dipolar couplings from the backbone region to predict possible deviations from the crystal structure that lead to a close fit to the data. Here we do not have this information. However, given the initial qualitative agreement with the rigid structure model and the precedent, it is clear that small rotations about torsions connecting the backbone and the acyl chain carbonyls could easily further scale down predicted offsets to magnitudes more consistent with the observed values. We therefore have at least some additional qualitative support for our initial choice of director orientation.

Conformation of the glycosidic linkage in solution

Three bond heteronuclear scalar couplings between carbons and protons on opposite sides of the glycosidic linkage can in principle report on average torsion angles ϕ and ψ as they are sampled in solution. We have been able to measure two of these using HSQC optimized to yield cross-peaks for spins connected by small couplings. $^3J_{C1'\text{-}H1}$ and $^3J_{C1\text{-}H1'}$ were measured for SQDG in CD_3OD (Table 3). The third relevant coupling $^3J_{C1\text{-}H1'}$ could not be accurately measured because of a low signal-to-noise ratio, but is likely to be significantly less than 4 Hz.

Fractional populations of low-energy conformations can be determined that are in agreement with the experimentally measured values. The populated conformations were taken as the low-energy regions of molecular modeling energy maps produced in the absence of a membrane potential (Fig. 6a). Four ϕ/ψ combinations correspond to low-energy regions; listed from lowest to highest, they are approximately I (ϕ = sc, ψ = −sc), II (ϕ = sc, ψ = ap), III (ϕ = sc, ψ = sc), and IV (ϕ = −sc, ψ = ap). Values for coupling constants corresponding to these minima were taken from a study on three-bond C-O-C-H carbon-proton long-range coupling constants in carbohydrates (Tvaroska et al., 1989). The relatively large value for $^3J_{C1'\text{-}H1}$ turns out to be the most significant. A mix of the three lowest energy minima that all have ϕ = sc (where C1′-O-C1-H1 is *gauche*, $^3J_{CH}$ = 1.625) cannot fit the observed values. Mixing in conformation IV, where C1′-O-C1-H1 is *trans* ($^3J_{CH}$ = 6.8), is necessary to reproduce observed couplings. A mix of three of the minima that can predict the observed coupling constants and keep the unmeasured $^3J_{C1\text{-}H1'}$ at a minimum is 52% I, 2% II, 46% IV. Small amounts of III may replace small amounts of II as one allows the unmeasured coupling to increase.

TABLE 3 Vicinal scalar coupling constants for 26% ^{13}C SQDG in CD_3OD at 313°K

Atom pair	^3J (Hz)	Torsion
Glycosidic linkage		
C1′, H1	4.0	C1′-O-C1-H1
C1, H1′	4.3	C1-O-C1′-H1′

DISCUSSION

From the results presented above, we have been able to derive structural and dynamic descriptions both in solution and bound to a membrane, of a naturally occurring glycolipid that has the intriguing property of inhibiting the cytopathic effects of HIV-1. Comparison of these results with our recently published studies on two other diacylglycerol glycolipids is appropriate.

We recently published detailed NMR/molecular modeling studies of the two most abundant diacylglycerol glycolipids, MGDG (Howard and Prestegard, 1995) and DGDG (Howard and Prestegard, 1996). Despite initial concern that the negative charge on SQDG would disrupt the composition and orientation properties of the DMPC/CHAPSO system, SQDG, MGDG, and DGDG oriented under very similar conditions. We did, however, detect a higher degree of order for the DMPC/CHAPSO discs incorporated with SQDG ($S_{bilayer}$ = 0.65) than the magnetically oriented DMPC/CHAPSO samples embedded with MGDG or DGDG ($S_{bilayer}$ = 0.51). The increase in order was seen in both the ^{31}P shift of DMPC and the CSA offsets of the carbonyls of DMPC. It is likely that electrostatic repulsion makes disks embedded with SQDG cooperative at longer distances—hence the higher degree of order.

Membrane-bound description of SQDG

The description of the headgroup of membrane-bound SQDG is reminiscent of that of DGDG and MGDG in that it is extended away from the bilayer surface into the aqueous phase, permitting maximum hydration by water molecules. Extension of the sugar headgroup away from the bilayer surface has also been seen in other studies of glycolipids (Jarrell et al., 1987; Skarjune and Oldfield, 1982). Furthermore, the glycosidic torsion angles of our best-fit SQDG conformation (centered at ϕ = 65/ψ = 105) are consistent with crystal structures of α-glycosides (Jeffrey and Taylor, 1980), which exhibit a preference for the sc range for ϕ (using the IUPAC definition of ϕ = O5-C1-O1-C1′).

Although the dearth of information on the backbone of SQDG prevented a detailed description of this region, it is interesting to compare the CSA offsets of SQDG with those measured for other diacylglycerol glycolipids. Whereas the CSA offsets for MGDG (−5.1 ± 1.2 ppm and −2.1 ± 1.2 ppm) and DGDG (−5.0 ± 1.2 ppm and −1.2 ± 1.2 ppm) were very similar, the sign of one of the SQDG CSA offsets differs (−4.2 ± 1.0 and +1.3 ± 1.0 ppm), indicating that the backbone conformation and/or dynamics of SQDG differ from those seen for MGDG and DGDG. The differences seen between these lipids is not surprising, considering that MGDG and DGDG both involve a β-link to the glycerol

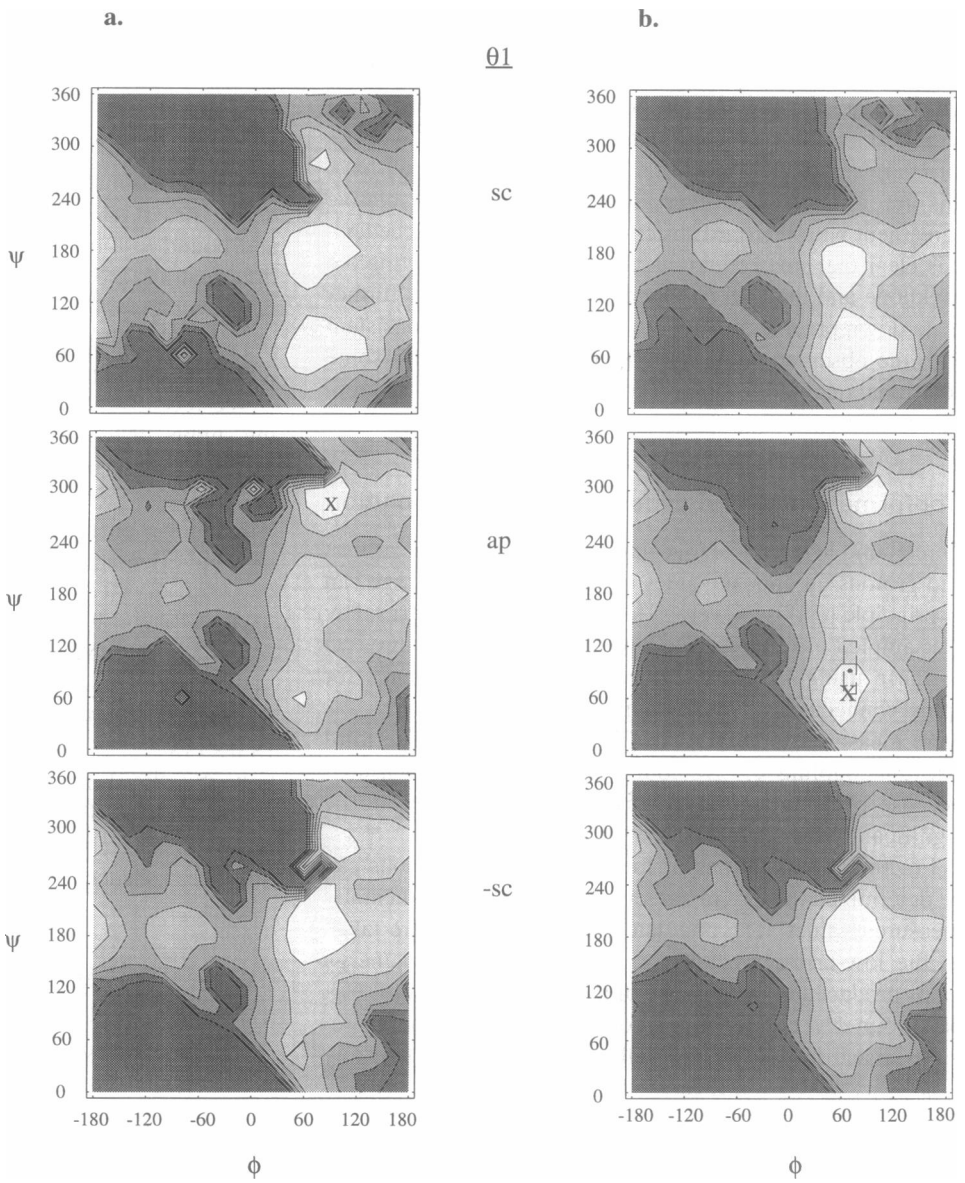

FIGURE 6 (*a*) Potential energy maps for SQDG in solution as a function of ϕ, ψ, and $\theta 1$. The global minimum is marked with an X. Contours are 2.3 kcal/mol apart. The darkest shaded area is the highest energy region and is at least 13.5 kcal/mol higher in energy than X. The four (ϕ/ψ) combinations that correspond to low-energy regions are referred to in the text as I (ϕ = sc, ψ = −sc), II (ϕ = sc, ψ = ap), III (ϕ = sc, ψ = sc), and IV (ϕ = −sc, ψ = ap). (*b*) Potential energy maps for membrane-bound SQDG as a function of ϕ, ψ, and $\theta 1$. The global minimum is marked with an X. The rectangle encompasses conformations within the range of motion for the best-fit membrane-bound solution described in footnote # of Table 2. Contours are 2.3 kcal/mol apart. The darkest shaded area is the highest energy region and is at least 13.5 kcal/mol higher in energy than X.

backbone, whereas SQDG has an α-link as well as a charged sulfonic acid group at the 6 position of the pyranose ring. It may be that the combination of the charge and the more restrictied α-link requires an adjustment in diacylglycerol motion and orientation. This variation in backbone behavior among these diacylglycerol glycolipids is at variance with a previous assertion made by Jarrell and coworkers that glycerol backbone properties were common to all glycerolipids and were determined by the lipid lattice rather than the headgroup regions (Jarrell et al., 1987). However, the sulfolipid is far from typical in many respects.

Solution conformation of SQDG

The number of transglycosidic couplings measured for SQDG is not adequate to give a definitive picture of conformational properties in solution. However, it is clear that conformer IV, with ϕ = −sc, ψ = ap, must be substantially populated in solution, whereas it is not populated when anchored to a membrane phase. Thus, in solution, more extensive motional averaging is involved than for the model consistent with the headgroup conformation of SQDG embedded in the lipid matrix. The restriction upon membrane association is also consistent with our finding for MGDG (Howard and Prestegard, 1995). Saccharides have been shown to sample a variety of conformations in solution (van Halbeek and Poppe, 1992). Oligosaccharides may be more ordered at the surface of a membrane because the lipid bilayer environment represents a condensed phase in which conformational interconversion could be energetically less favorable because of steric hindrance, or because of specific intermolecular hydrogen bonding with neighboring molecules.

Modeling of SQDG

In an effort to systematically model the effects of the membrane surface on glycolipid headgroups, potential energy maps as a function of glycosidic torsions were calculated both with and without a membrane interaction energy for SQDG. Fig. 6 shows two sets of energy maps, one without and one with a membrane interaction energy. Each set includes three maps, one for each of the staggered conformations of $\theta 1$. Fig. 6 *a* was introduced in the Results section in the analysis of vicinal scalar couplings for solution data. The energy map set in Fig. 6 *b* is calculated with the same modeling protocol as the set in Fig. 6 *a*, except for the addition of the membrane interaction energy. The global minimum of each set of maps is noted with an X. The dashed box in Fig. 6 *b* indicates the range of motion of the best-fit solution to the membrane-bound data.

The overall shapes of the two sets of maps, with and without membrane energy, are similar. However, the addition of the membrane energy does change the relative depth and width of the minima. The membrane interaction energy stabilizes structures at the $\psi = 60$ strip of the ϕ/ψ maps that extend away from the membrane surface. Addition of the membrane interaction energy moves the global minimum from ϕ = sc/ψ = −sc to ϕ = sc/ψ = sc, where $\theta 1$ is ap. With the addition of the membrane energy, the model consistent with the liquid crystal data now coincides with the apparent global minimum. Inclusion of the membrane interaction term, therefore, clearly improves agreement between experimental and theoretical solutions. This was also true for our study of MGDG (Howard and Prestegard, 1995). However, the total energies were vastly different between MGDG (a few kcal/mol) and SQDG (around −450 kcal/mol), with the larger energies for SQDG primarily due to the dipoles associated with the sulfonic acid moiety. Difficulties in modeling solvent interactions with highly polar, much less charged groups are well recognized. Because our modeling of the sulfonic acid portion of the molecule is very crude, the absolute magnitudes of the SQDG energies should be viewed with some skepticism. However, the qualitative variation in the membrane interaction energy from one part of the ϕ/ψ conformational maps to the other should be realistic. In both MGDG and SQDG cases the membrane interaction energies serve to stabilize some regions over others by a similar magnitude. Because of differences in structure, the regions of the ϕ/ψ maps with the most stabilizing membrane energy are different. For MGDG, a β-linked sugar, conformers with ψ near 180 are stabilized. For SQDG, an α-linked sugar, conformers with ψ near 60 are stabilized. However, the respective stabilized regions both extend the headgroup away from the membrane surface.

NMR studies of magnetically oriented membrane fragments presented here therefore prove successful in describing the membrane-bound conformation of an interesting charged glycolipid at a simple lipid interface. The conformation that membrane-bound SQDG adopts on interaction with a protein essential to viral proliferation and/or cytotoxity may be even more interesting. Some previous studies with proteins bound to glycolipids have been successfully conducted using magnetically oriented membranes (Aubin et al., 1993; Hare et al., 1994). This offers promise that the work presented here could be extended to the study of complexes of SQDG with other molecules as these molecules are identified.

This work was supported by National Institutes of Health grant GM33225.

REFERENCES

Allinger, N. L., and J. Kao. 1976. Molecular mechanics studies of sulfoxides. *Tetrahedron.* 32:529–536.

Aubin, Y., Y. Ito, J. C. Paulson, and J. H. Prestegard. 1993. Structure and dynamics of the sialic acid moiety of the GM3-ganglioside at the surface of a magnetically oriented membrane. *Biochemistry.* 32:13405–13413.

Auger, M., M. Van Calsteren, I. C. P. Smith, and H. C. Jarrell. 1990. Glycerolipids: common features of molecular motion in bilayers. *Biochemistry.* 29:5815–5821.

Barber, J., and K. Gounaris. 1986. What role does sulpholipid play within the thylakoid membrane? *Photosynth. Res.* 9:239–249.

Bax, A., R. H. Griffey, and B. L. Hawkins. 1983. Correlation of proton and nitrogen-15 chemical shifts by multiple quantum NMR. *J. Magn. Res.* 55:301–315.

Bax, A., and M. F. Summers. 1986. ^{1}H and ^{13}C assignments from sensitivity-enhanced detection of heteronuclear multiple-bond connectivity by 2D multiple quantum NMR. *J. Am. Chem. Soc.* 108:2093–2094.

Benson, A., H. Daniel, and R. Wiser. 1959. A sulfolipid in plants. *Proc. Natl. Acad. Sci. USA.* 45:1582–1587.

Bodenhausen, G., and D. J. Ruben. 1980. Natural abundance nitrogen-15 NMR by enhanced heteronuclear spectroscopy. *Chem. Phys. Lett.* 69: 185–189.

Braach-Maksvytis, V. L. B., and B. A. Cornell. 1988. Chemical shift anisotropies obtained from aligned egg yolk phosphatidylcholine by solid-state ^{13}C nuclear magnetic resonance. *Biophys. J.* 53:839–843.

Cornell, B. A. 1980. The dynamics of the carbonyl groups in phospholipid bilayers from a study of their ^{13}C chemical shift anisotropy. *Chem. Phys. Lett.* 72:462–465.

Cornell, B. A. 1986. Chemical shielding tensors of ^{13}C in solid dimethyl oxalate. *J. Chem. Phys.* 85:4199–4201.

Gordon, D., and S. Danishefsky. 1991. Synthesis of a cyanobacterial sulfolipid: conformation of its structure, stereochemistry and anti-HIV-1 activity. *J. Am. Chem. Soc.* 114:659–663.

Gosser, Y., K. Howard, and J. Prestegard. 1993. Three-dimensional ^{1}H-detected ^{13}C-^{13}C correlation experiments for carbon backbone assignments of enriched natural products. *J. Magn. Res. B.* 101:126–133.

Gounaris, K., and J. Barber. 1985. Isolation and characterisation of a photosystem II reaction centre lipoprotein complex. *FEBS Lett.* 188: 68–72.

Gustafson, K., J. Cardellina, R. Fuller, O. Weislow, R. Kiser, K. Snader, G. Patterson, and M. Boyd. 1989. AIDS-antiviral sulfolipids from cyanobacteria (blue-green algae). *J. Natl. Cancer Inst.* 81:1254–1258.

Hare, B. J., K. P. Howard, and J. H. Prestegard. 1993. Torsion angle analysis of glycolipid order at membrane surfaces. *Biophys. J.* 64: 392–398.

Hare, B. H., F. Rise, Y. Aubin, and J. H. Prestegard. 1994. ^{13}C NMR studies of wheat germ agglutinin interactions with *N*-acetylglucosamine at a magnetically oriented bilayer surface. *Biochemistry.* 33: 10137–10148.

Harris, R. 1983. Nuclear Magnetic Resonance Spectroscopy. John Wiley, New York.

Harwood, J. 1980. Sulfolipids. *In* The Biochemistry of Plants. P. Stumpf, editor. Academic Press, New York. 301–320.

Howard, K., and J. Prestegard. 1995. Membrane and solution conformations of monogalactosyldiacylglycerol using NMR/molecular modeling methods. *J. Am. Chem. Soc.* 117:5031–5040.

Howard, K., and J. Prestegard. 1996. NMR studies of the conformation and dynamics of membrane-bound digalactosyldiacylglycerol. *J. Am. Chem. Soc.* 118:3345–3353.

Jarrell, H. C., P. A. Jovall, J. B. Giziewicz, L. A. Turner, and I. C. P. Smith. 1987. Determination of conformational properties of glycolipid head groups by ^{2}H NMR of oriented multibilayers. *Biochemistry.* 26: 1805–1811.

Jeffrey, G. A., and R. Taylor. 1980. The application of molecular mechanics to the structures of carbohydrates. *J. Comp. Chem.* 1:99–109.

Johns, S., R. Leslie, R. Willing, and D. Bishop. 1978. Studies on chloroplast membranes. III. ^{13}C chemical shifts and longitudinal relaxation times of 1,2-diacyl-3-(6-sulphoquinovosyl)sn-glycerol. *Aust. J. Chem.* 31:65–72.

Kogelberg, H., and T. J. Ruitherford. 1994. Studies on the three-dimensional behavior of the selectin ligands Lewis(a) and sulfated Lewis(a) using NMR spectroscopy and molecular dynmaics simulation. *Glycobiology.* 4:49–57.

Lamba, D., S. Glover, W. Mackie, A. Rashid, B. Sheldrick, and S. Perez. 1994. Insights into stereochemical features of sulphated carbohydrates: X-ray crystallographic and modelling investigations. *Glycobiology.* 4:151–163.

Mareci, T. H., and R. Freeman. 1982. Echoes and antiechoes in coherence transfer NMR: determining the signs of double-quantum frequencies. *J. Magn. Res.* 48:158–163.

McAlarney, T., S. Apostolski, S. Lederman, and N. Latov. 1994. Characteristics of HIV-1 gp120 glycoprotein binding to glycolipids. *J. Neurosci. Res.* 37:453–460.

McClure, M., J. Moore, D. Blanc, P. Scotting, G. Cook, R. Keynes, J. Weber, D. Davies, and R. Weiss. 1992. Investigations into the mechanism by which sulfated polysaccharides inhibit HIV infection in vitro. *AIDS Res. Hum. Retroviruses.* 8:19–26.

Nyholm, P., and I. Pascher. 1993. Orientation of the saccharide chains of glycolipids at the membrane surface: conformational analysis of the glucose-ceramide and the glucose-glyceride linkages using molecular mechanics (MM3). *Biochemistry.* 32:1225–1234.

Okaya, Y. 1964. The plant sulfolipid: a crystallographic study. *Acta. Crystallogr.* 17:1276–1282.

Pascher, I., M. Lundmark, P. Nyholm, and S. Sundell. 1992. Crystal structures of membrane lipids. *Biochim. Biophys. Acta.* 1113:339–373.

Pearson, R. H., and I. Pascher. 1979. The molecular structure of lecithin dihydrate. *Nature.* 281:499–501.

Pick, U., K. Gounaris, M. Weiss, and J. Barber. 1985. Tightly bound sulpholipids in chloroplast CF0-CF1. *Biochim. Biophys. Acta.* 808: 415–420.

Ram, P., E. Kim, D. S. Thomson, K. P. Howard, and J. H. Prestegard. 1992. Computer modeling of glycolipids at membrane surfaces. *Biophys. J.* 63:1530–1535.

Rance, M., O. W. Sorensen, G. Bodenhausen, G. Wagner, R. R. Ernst, and K. Wuthrich. 1983. Improved spectral resolution in COSY ^{1}H NMR spectra of proteins via double quantum filtration. *Biochem. Biophys. Res. Commun.* 117:479–485.

Sanders, C. R., B. J. Hare, K. P. Howard, and J. H. Prestegard. 1994. Magnetically oriented phospholipid micelles as a tool for the study of membrane-associated molecules. *Prog. NMR Spectrosc.* 26:421–444.

Sanders, C. R., and J. H. Prestegard. 1990. Magnetically orientable phospholipid bilayers containing small amounts of a bile salt analoque, CHAPSO. *Biophys. J.* 58:447–460.

Sanders, C. R., and J. H. Prestegard. 1991. Orientation and dynamics of β-dodecyl glucopyranoside in phospholipid bilayers by oriented sample NMR and order matrix analysis. *J. Am. Chem. Soc.* 113:1987–1996.

Sanders, C. R., and J. H. Prestegard. 1992. Headgroup orientations of alkyl glycosides at a lipid bilayer interface. *J. Am. Chem. Soc.* 114: 7096–7107.

Sato, N., and N. Murata. 1988. Membrane lipids. *Methods Enzymol.* 167:251–259.

Scarsdale, J. N., P. Ram, and J. H. Prestegard. 1988. A molecular mechanics-NMR pseudoenergy approach to the solution conformation of glycolipids. *J. Comp. Chem.* 9:133–147.

Shaka, A., J. Keeler, and R. Freeman. 1983. Evaluation of a new broadband decoupling sequence: WALTZ-16. *J. Magn. Res.* 53:313–340.

Siebert, H., G. Reuter, R. Schauer, C. von der Lieth, and J. Dabrowski. 1992. Solution conformations of GM3 gangliosides containing different sialic acid residues as revealed by NOE-based distance mapping, molecular mechanics, and molecular dynamics calculations. *Biochemistry.* 31:6962–6971.

Skarjune, R., and E. Oldfield. 1982. Physical studies of cell surface and cell membrane structure. Deuterium NMR studies of N-palmitoylglucosylceramide (cerebroside) head group structure. *Biochemistry.* 21: 3154–3160.

Smith, S. O., I. Kustanovich, S. Bhamidipati, A. Salmon, and J. A. Hamilton. 1992. Interfacial conformation of dipalmitoylglycerol and dipalmitoylphosphatidylcholine in phospholipid bilayers. *Biochemistry.* 31:11660–11664.

Still, W. C. 1990. Macromodel V3.1. Department of Chemistry, Columbia University, New York.

Strenk, L. M., P. W. Westerman, and J. W. Doane. 1985. A model of orientational ordering in phosphatidylcholine bilayers based on conformational analysis of the glycerol backbone region. *Biophys. J.* 48: 765–773.

Tvaroska, I., M. Hricovini, and E. Petrakova. 1989. An attempt to derive a new Karplus-type equation of vicinal proton-carbon coupling constants for C-O-C- H segments of bonded atoms. *Carbohydr. Res.* 189: 359–362.

Van den Berg, L., S. Sadiq, S. Lederman, and N. Latov. 1992. The gp120 glycoprotein of HIV-1 binds to sulfatide and to the myelin associated glycoprotein. *J. Neurosci. Res.* 33:513–518.

van Halbeek, H., and Poppe, L. 1992. Conformation and dynamics of glycoprotein oligosaccharides as studied by ^{1}H NMR spectroscopy. *Magn. Reson. Chem.* 30:S74–S86.

Vanderkooi, G. 1991. Multibilayer structure of dimyristoylphosphatidylcholine dihydrate as determined by energy minimization. *Biochemistry.* 30:10760–10768.

Weiner, S. J., P. A. Kollman, D. A. Case, U. C. Singh, C. Ghio, G. Alogona, S. Profeta, P. J. Weider. 1984. A new force field for molecular mechanical simulation of nucleic acids and proteins. *J. Am Chem. Soc.* 106:765.

Weiner, S. J., P. A. Kollman, D. T. Nguyen, and D. A. Case. 1986. An all atom force field for simulations of proteins and nucleic acids. *J. Comp. Chem.* 7:230–252.

Weislow, O., R. Kiser, D. Fine, J. Bader, B. Shoemaker, and M. Boyd. 1989. New soluble-formazan assay for HIV-1 cytopathic effects: application to high flux screening of synthetic and natural products for AIDS-antiviral activity. *J. Natl. Cancer Inst.* 81:577–586.

Winsborrow, B. G., J. Brisson, I. C. P. Smith, and H. C. Jarrell. 1992. Influence of the membrane surface on glycolipid conformation and dynamics. *Biophys. J.* 63:428–437.